



# A novel model to evaluate spatial structure in thinned conifer-broadleaved mixed natural forests

Hui Liu<sup>1</sup> · Xibin Dong<sup>1</sup> · Yuan Meng<sup>1</sup> · Tong Gao<sup>1</sup> ·  
Liangliang Mao<sup>1</sup> · Ran Gao<sup>1</sup>

Received: 8 May 2023 / Accepted: 23 May 2023 / Published online: 11 August 2023  
© The Author(s) 2023

**Abstract** In order to ensure the effective analysis and reconstruction of forests, it is key to ensure the quantitative description of their spatial structure. In this paper, a distance model for the optimal stand spatial structure based on weighted Voronoi diagrams is proposed. In particular, we provide a novel methodological model for the comprehensive evaluation of the spatial structure of forest stands in natural mixed conifer-broadleaved forests and the formulation of management decision plans. The applicability of the rank evaluation and the optimal solution distance model are compared and assessed for different standard sample plots of natural mixed conifer-broadleaved forests. The effect of crown width on the spatial structure unit of the trees is observed to be higher than that of the diameter at breast height. Moreover, the influence of crown length is greater than that of tree height. There are nine possible spatial structure units determined by the weighted Voronoi diagram for the number of neighboring trees in the central tree, with an average intersection of neighboring crowns reaching 80%.

The rank rating of natural forest sample plots is correlated with the optimal solution distance model, and their results are generally consistent for natural forests. However, the rank rating is not able to provide a quantitative assessment. The optimal solution distance model is observed to be more comprehensive than traditional methods for the evaluation of the spatial structure of forest stands. It can effectively reflect the trends in realistic stand spatial structure factors close to or far from the ideal structure point, and accurately assesses the forest spatial structure. The proposed optimal solution distance model improves the integrated evaluation of the spatial structure of forest stands and provides solid theoretical and technical support for sustainable forest management.

**Keywords** Weighted Voronoi diagram · Optimal distance model · Spatial structure quantification · Thinning intensity · Conifer-broadleaved mixed natural forests

## Introduction

The high spatial structure heterogeneity of forests is considered to have a positive impact on the characteristics and functions of ecosystems, including biodiversity, resilience, and adaptability, and to a large extent determines the competition between trees and the spatial niche. It also reflects the health status, growth potential, and stability of the stand (Brang 2005; Nagel and Svoboda 2008; Nagel et al. 2013). The function of a stand depends on the heterogeneity level of the spatial structure of the stand, namely, how ideal the forest spatial structure is (Song and Dong 2014; Pommerening 2006). In natural mixed secondary forests, the spatial structure of the forest is often optimized through thinning methods. Thus, the high heterogeneity of the forest spatial structure is often imitated in forest management.

Project funding: This study was funded by National Key Research and development project (2022YFD2201001).

The online version is available at <https://link.springer.com>.

Corresponding editor: Yu Lei.

**Supplementary Information** The online version contains supplementary material available at <https://doi.org/10.1007/s11676-023-01647-w>.

✉ Xibin Dong  
xibindong@nefu.edu.cn

<sup>1</sup> Key Laboratory of Sustainable Forest Management and Environmental Microorganism Engineering of Heilongjiang Province, Northeast Forestry University, Harbin 150040, People's Republic of China

This management method not only enhances self-recovery (Knocke et al. 2008) and improves the forest environment (Zhang et al. 2023; Cascone et al. 2021), but also affects the diameter at breast height, tree height, crown length, and crown width (i.e., the forest non-spatial structure) (Gauthier and Tremblay 2019; Horner et al. 2010), as well as the distribution pattern degree, mingling, and the competition of forest trees within stands (i.e., the forest spatial structure) (Duchateau et al. 2021; Ye et al. 2018).

The quantitative evaluation of stand spatial structure plays a key role in the development of the highly heterogeneous spatial structure in natural mixed conifer-broadleaved forests under thinning practices. Qualitative grade and homogeneity index evaluations are often used for the evaluation of stand spatial structures (Li et al. 2020; Xin et al. 2020; Yang et al. 2019). Qualitative ranking assigns a rank to each parameter of the spatial structure, while homogeneity index evaluates the overall level of a certain stand characteristic based on mean value. Nevertheless, there are quite a few limitations of these methods in quantifying composite indicators and neglecting the distribution of spatial structure indicators, which may bias potentially in the results. The ideal angle for each spatial structure unit in a stand would be 0.5, with a mean value of 0.5. However, if half of the stands are rated as 1 and the other half as 0, the mean value would still be 0.5. Despite not reaching the ideal state as no stand is in an ideal condition. Furthermore, the most important index in the study of spatial structure parameters is still controversial. It is the value to be taken for the number of nearest neighbor trees of the central tree. Non-nearest neighbors may be included in the calculation if the number of nearest neighbors is too large; All possible scenarios of nearest neighbors around the central tree cannot be accounted for the number of nearest neighbors is too small. The both of which lead to biased estimates of the spatial structure parameters (Tang et al. 2009).

Voronoi diagrams are used for the quantitative analysis of the spatial structure of forest stands due to their nearest-neighbor and neighbor properties. In order to express the degree of spatial segregation of tree species in terms of mingling, Mengping Tang (Tang et al. 2009) employed Voronoi diagrams to determine the number of nearest neighbors,  $n$ , overcoming the overestimation of mingling caused by too large or too small a value of  $n$ . The Delaunay diagram is a Voronoi dual structure that is based on a minimum angle maximization principle, namely, every two adjacent triangles form the diagonal of a convex quadrilateral, and the minimum angle of the six interior angles does not increase after mutual exchange. This maximizes the equilibrium and avoids narrow triangles. Each triangular side length in the triangular network corresponds to the distance between adjacent trees. This structure can better reflect the distribution pattern of the horizontal ground. However, the standard

Voronoi diagram assumes that trees are equally weighted. Nevertheless, in reality, there exist differences in the diameter at breast height, tree height, crown width and crown length of each tree, which results in various competitiveness between trees. Consequently, different competitive units were formed. Therefore, it is necessary to correct the standard Voronoi diagram with non-spatial structural features (Li et al. 2015; Aakala et al. 2013; Abellanas et al. 2016; Cao and Li 2016).

This study had two objectives. First, the parameters of the spatial structure of the stand derived from the weighted Voronoi diagram were compared with the results calculated by traditional methods; second, the quantitative evaluation of the spatial structure of the stand was compared with the results of the rank evaluation. The weighted Voronoi diagram proposed in this study allows for the effective selection of adjacent trees, while the subjective and objective combination of weights can determine the importance of the spatial structure parameters of the stand, and the optimal solution distance theory corrects for the data bias associated with the mean value of the spatial structure index. This method has recently been applied in the supply chain, environment, energy, business, wood traits and healthcare management systems (Palczewski and Sařabun 2019; Irfan et al. 2022; dos Santos et al. 2019; Solangi et al. 2021; Zhang et al. 2022) and is fundamentally based on the distance model, which assumes that the real state is far from or approximates the trend of the ideal state (Wang and Li 2004; Qiao et al. 2020; Yang et al. 2021). This theory of distance has effectively been employed to evaluate forest ecosystem health (Chen et al. 2004; Lodin and Brukas 2021; Abedi 2022) and in the qualitative analysis of forest spatial structure (Dong et al. 2022).

## Materials and methods

### Study area

The study area was located in the Dailing Forestry Experimental Bureau at Dongfanghong Forest Farm in the Lesser Khingan Mountains of Heilongjiang Province, China (128°37'46" to 129°17'50"E, 46°50'8" to 47°21'32"N), at an average elevation of 600 m. The forest community was a conifer-broad mixed secondary forest, and the main tree species were *Pinus koraiensis* Sieb. et Zucc, *Picea koraiensis* Nakai, *Abies nephrolepis* Maxim, *Tilia amurensis* Rupr., *Betula platyphylla* Suk., and *Fraxinus mandshurica* Rupr..

In 2011, natural conifer-broadleaved mixed forests with the same stand density were selected in the study area and subjected to lower story thinning. The harvested trees were non-target species, partially over-dense trees, and harmful species, including diseased, decayed, stressed, and dying

trees, as well as trees with poor trunk shapes. The inter-harvesting intensity was determined using the ratio of the harvested forest cumulative quantity to the total forest cumulative quantity. A total of seven 100 m × 100 m test plots were established, namely, 10%, 15%, 20%, 25%, 30%, and 35% thinning intensity plots and a plot with thinning exclusion. The average age, diameter at breast height, and tree height of the trees in the study sites were 70 a, 13.5 cm and 10.5 m, respectively, and the stand canopy densities were above 0.8 before thinning. In 2021, we measured the height, diameter at breast height (≥ 5 cm), live branch height, crown width, crown length, species and coordinates for over 800 trees at seven 30 m × 40 m standard plots. These characteristics are summarized in Table 1. The standard plots have an average level representative of the total stand characteristics (Li 2019).

**Determination of spatial structure units and selection of structural parameters**

*Determination of spatial structure units*

The non-spatial structure of trees can lead to varying responses to thinning, for example, removing part of the over-dense trees may result in crown gaps, reduce competition for light by the remaining trees and ameliorate light availability. This may result in changes in diameter at breast height (DBH), tree height and so on, and consequently, different competitiveness between trees.

Based on the nearest neighbor property of Voronoi diagrams, we define  $P_i (i = 1, 2, \dots, n)$  as  $n$  points in a two-dimensional Euclidean space and  $\lambda_i (i = 1, 2, \dots, n)$  as  $n$  positive real numbers. The regular Voronoi diagram is a special case of the weighted Voronoi diagram with equal weights, namely,  $\lambda_1 = \lambda_2 = \dots = \lambda_n$ . However, the actual central tree in our study differed from the surrounding adjacent trees owing to its stand properties (diameter at breast height, tree height, crown length, and crown width), which results in varying effects (i.e., competitive range). For example, stand 82 of the conventional Voronoi diagram in Fig. 1b is

hexagonal without weighting, whereas stand 82 is pentagonal after weighting (as in Fig. 1c), namely central tree 82 has five adjacent trees, 81, 84, 83, 79 and 77. Each weighted Voronoi diagram is a polygon, and each edge of the polygon corresponds to an adjacent tree of the central tree. Moreover, the number of edges of the weighted Voronoi polygon corresponded to the number of neighbors of the central tree. Thus, the white areas connected with 82 in Fig. 1c denote the influence range of central tree 82.

The weighted Voronoi diagram was used to determine adjacent trees. The outer boundary of the Voronoi polygon was taken as the area where all four edges of the original forest plot widened horizontally by 2 m, while the distance buffer method was employed to eliminate the influence of edges. Furthermore, the buffer region of the Voronoi polygon was selected as the area where all four edges of the original forest plot indented horizontally by 2 m. The corrected sample plot was thus the remainder of the sample plot with the buffer zone removed. We take the weighted Voronoi diagram of the forest plot with thinning exclusion as an example (Fig. 1a). The trees in the corrected forest plots were employed as the central trees to calculate each spatial structure index, while those in the buffer zone were only used as adjacent trees in the calculation. Delaunay triangular nets were adopted to avoid exaggerating the influence of adjacent trees on the central tree, thus preventing excessive distances between the central and adjacent trees in spatial structural units.

We adopted grey theory to determine the degree of influence and relationship between factors by calculating the similarity between the geometry of the reference and comparison sequence. Grey systems theory, which employs grey correlation analysis, does not require a large amount of complete information to deal with non-linear problems. We used the entropy-grey correlation method to analyze the intrinsic relationship between the number of convex edges in the Voronoi diagram and the corresponding diameter at the breast height, height, crown width, and crown length of the trees and assigned weights to the diameter at breast height, height, crown width, and crown length. Grey correlation analysis was

**Table 1** Characteristics of the forest plot surveyed

Thinning intensity (%)	Stand density (ind·ha <sup>-1</sup> )	No. of trees surveyed	No. of trees in corrected plot	Mean DBH (cm)	Average height (m)	Average crown breadth (m)
0	1233	148	120	11.65	12.14	4.65
10	833	100	75	15.36	12.95	6.97
15	1000	120	85	15.14	12.60	5.85
20	758	91	66	16.14	11.77	4.63
25	1058	127	97	14.36	11.14	4.56
30	975	117	98	13.38	12.18	5.34
35	983	118	94	14.74	13.74	5.29

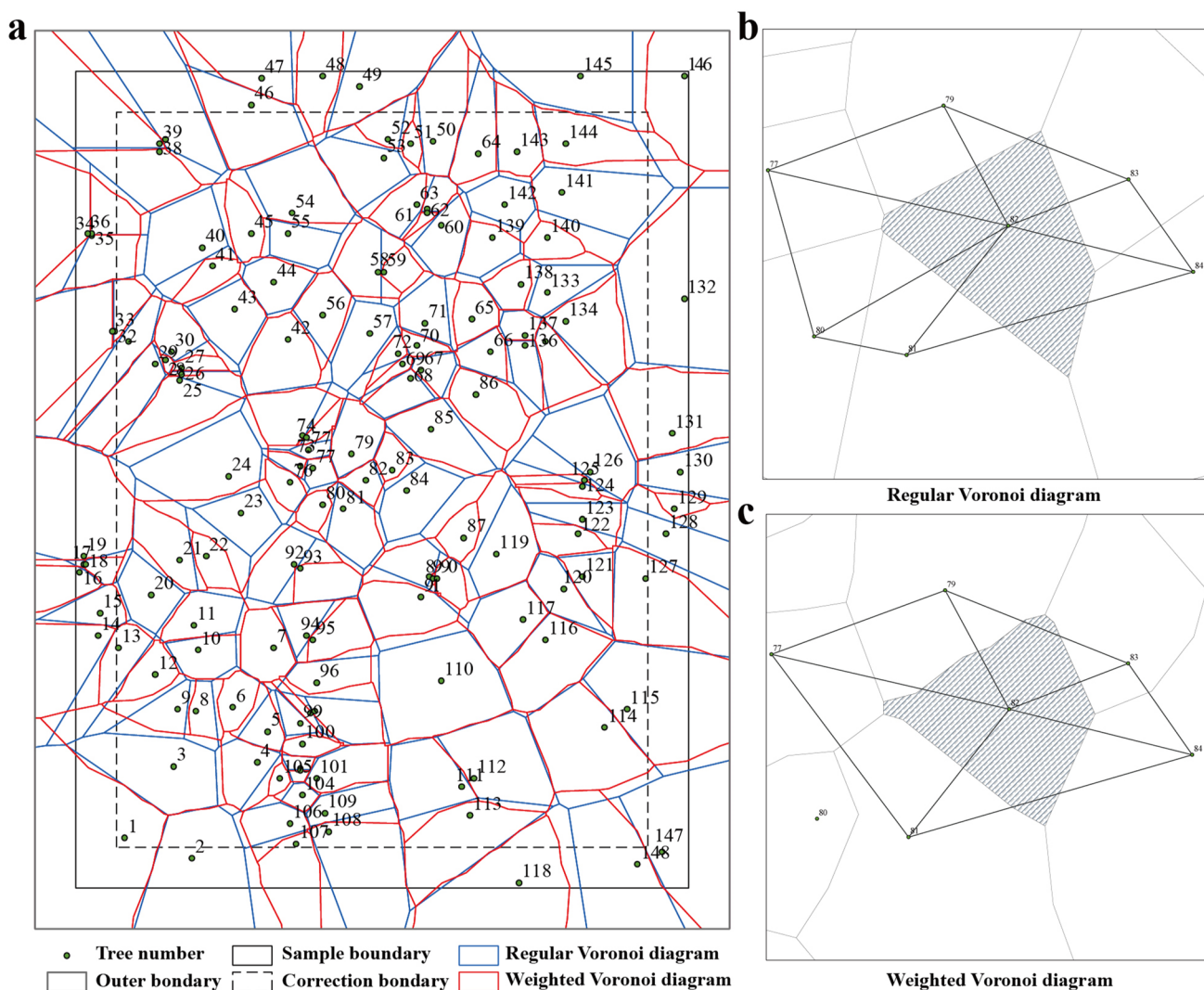


**Fig. 1** Weighted Voronoi diagram after correcting forest plot edges

used to consider the number of trees adjacent to the central tree and the characteristics of the stand’s attributes as a grey system, and analyze the influence of each stand’s attributes on the number of adjacent trees. The number of trees adjacent to the central tree was used as reference series  $X_0$ , while the factors influencing the number of trees adjacent to the central tree (i.e., diameter at breast height, height, crown length, and average crown width of the central tree) were used as the comparator series. The correlation coefficient formula is as follows:

$$\varepsilon_i(k) = \frac{\Delta_{min} + \rho\Delta_{max}}{\Delta_i(k) + \rho\Delta_{max}} = \frac{\Delta_{min} + \rho\Delta_{max}}{|X_0(k) - X_i(k)| + \rho\Delta_{max}} \quad (1)$$

for  $X_i$ , where,  $i = 1, 2, 3, 4$ ;  $X_0 = [X_0(1), X_0(2), X_0(3), \dots, X_0(n)]$ ;  $X_i = [X_i(1), X_i(2), X_i(3), \dots, X_i(n)]$ ;  $n$  is the

number of the central tree;  $\Delta_i(k)$  is the absolute difference between sequence  $X_0$  and  $X_i$  at point  $k$ ;  $\Delta_{min}$  and  $\Delta_{max}$  denote the minimum and maximum absolute differences at each moment of all comparator series, respectively; and  $\rho$  is the discriminant coefficient used to weaken the distortion caused by the maximum absolute difference, namely, to increase the significance of the difference between the correlation coefficients.  $\rho$  varies between  $[0, 1]$  and is usually equal to 0.5 (Sun 2007). To facilitate comparisons, we use the critic method to weight each characteristic factor (i.e., to obtain the weighted correlation degree). The critical grey method not only evaluates the differences within a single indicator but also measures the correlation between indicators and subsequently determines each factor’s importance. The weighted grey correlation is obtained as follows.

**Table 2** Definition for each spatial structure index

Spatial structure	Formula	Detailed explanation	Value
$M_{vc}$	$M_{vc} = \frac{1}{2} \left( D_i + \frac{n_i}{n} \right) M_{vi}$	$M_{vi} = \frac{1}{n} \sum_{j=1}^n V_j; D_i = 1 - \frac{1}{(n+1)^2} \sum_{j=1}^{s_i} n_j^2$	0 (0, 0.25] (0.25, 0.5] (0.5, 0.75] (0.75, 1]
$OP_v$	$OP_{vi} = \frac{1}{n} \sum_{j=1}^n t_{ij}$	$V_{ij} = \begin{cases} 1 & \text{When } i \text{ and } j \text{ belong to different tree species} \\ 0 & \text{otherwise} \end{cases}$ $t_{ij} = \begin{cases} 1 & L_{ij} >  H_i - H_j  \\ 0 & \text{otherwise} \end{cases}$	Not mixed Weakly mixed Intermediately mixed Strongly mixed Extremely strongly mixed
$H_v$	$H_{vi} = \frac{s_i}{6} \frac{1}{n} \sum_{j=1}^n S_{ij}$	$S_{ij} = \begin{cases} 1 & \text{When } i \text{ and } j \text{ belong to the same forest layer} \\ 0 & \text{otherwise} \end{cases}$	Fully shaded Shaded Relatively open Extremely open
$W_v$	$W_{vi} = \frac{1}{n} \sum_{j=1}^n Z_{ij}$	$Z_{ij} = \begin{cases} 1 & a_{ij} < a_0; a_0 = 360^\circ / (n + 1) \\ 0 & a_{ij} \geq a_0 \end{cases}$	No difference Weak Uniform Nonuniform
$C_v$	$C_{vi} = \frac{1}{n} \sum_{j=0}^n y_{ij}$	$y_{ij} = \begin{cases} 1 & \text{When } i \text{ overlaps the crown of } j \\ 0 & \text{otherwise} \end{cases}$	Absolutely uniform Extremely sparse Moderately dense Relatively dense
$U_v$	$U_{vi} = \frac{1}{n} \sum_{j=1}^n k_{ij}$	$k_{ij} = \begin{cases} 1 & \text{DBH of } i \leq \text{DBH of } j \\ 0 & \text{otherwise} \end{cases}$	Predominant Subdominant Moderate Inferior
$aCI_v$	$aCI_{vi} = \frac{1}{n} \sum_{j=1}^n \frac{(\alpha_1 + \alpha_2 * c_{ij})}{180^\circ} c_{ij}$	$c_{ij} = \begin{cases} 1 & \text{if } H_j > H_i \\ 0 & \text{otherwise} \end{cases}$ $\alpha_1 = \begin{cases} \arctg(H_i/L_{ij}), \text{ if } H_j > H_i \\ \arctg(H_j/L_{ij}), \text{ otherwise} \end{cases}; \alpha_2 = \begin{cases} \arctg\left(\frac{H_i - H_j}{L_{ij}}\right) \\ \end{cases}$	Not competition Weakly competition Moderately competition Strongly competition Extremely strongly competition

$$r_i = \sum_{k=1}^n w_i \varepsilon_i(k) \tag{2}$$

The correlations between four factors—tree height, diameter at breast height, crown length, and average crown width—and the number of trees adjacent to the central tree were then calculated. The combined weights of the four factors were calculated as  $\lambda_i = \lambda_1 + \lambda_2 + \lambda_3 + \lambda_4$ . The weighted Voronoi diagram was generated using the Weighted Voronoi Diagram tool in ArcGIS10.5 (Esri) to determine the stand spatial structure units and calculate the stand spatial structure index.

*Selection of spatial structure parameters of forest stands*

The spatial structure of stands refers to the distribution pattern of trees and the spatial arrangement of their attributes. It determines the competitive potential, the spatial niche of the trees and, to a large extent, the size of the management space, the stability of the stand and the possibility of its development. Four key aspects form the basis of the spatial structure of stands: mingling, spatial distribution pattern, competition degree and degree of tree shade. Seven spatial structure parameters representing these four parameters were selected based on tree mingling, uniform angle, competition, neighborhood comparison, openness ratio, crowding, and forest layer difference for the structure analysis and evaluation. The aforementioned variables were adopted to represent the overall situation of stand spatial structure. Among them, the degree of species mingling ( $M_{vc}$ ) describes the degree of spatial isolation of the stand (Hui et al. 2019), the openness ratio ( $OP_v$ ) reflects the light transmission condition of the stand (Li et al. 2013), and the stand layer difference ( $H_v$ ) describes the vertical structure diversity of the stand (Lv et al. 2012). The uniform angle ( $W_v$ ) expresses the spatial distribution pattern of trees, crowding ( $C_v$ ) reflects the degree of intersection of the tree crowns, and neighborhood comparison ( $U_v$ ) reflects the degree of size differentiation based on the DBH. Lastly, the competition index ( $aCI_v$ ) expresses the intensity of competition among trees (Hui et al. 2013). The specific formulae and the explanation of the values are described in Table 2 and Supplementary Material Tables S1 – S8. The range of each parameter is divided into five intervals, namely, 0.00, (0.00, 0.25], (0.25, 0.50], (0.50, 0.75], and (0.75, 1.00]. Among them, the forest layer is divided into six levels based on the Technical Regulations for the Inventory for Forest Management Planning and Design, National Standard of the People’s Republic of China GB/T 26424–2010. Moreover, trees within the 2-m buffer zone were used as reference trees to determine the spatial structure parameters.

$D_i$  represents the first  $i$  diversity index values of all tree species within the basic spatial structure unit in which the central tree is located. The central tree is represented by  $z_i$ , where  $i$  represents the number of forest layers in the spatial structure unit;  $a_{ij}$  represents the angle between the line of two directly adjacent trees and the central tree, and  $a_0$  represents the standard angle of the structural unit.  $H_i, H_j, L_{ij}, n, i$ , and  $j$ , represent the height of the central tree, the height of adjacent trees, the horizontal distance between the central tree and adjacent trees, the number of adjacent trees in the spatial structure unit, the central tree, and the adjacent trees, respectively. The number of tree species in the structural unit is denoted as  $n_i$ , while  $n_j$  represents the number of the  $j$ th tree species in the structure unit in which the  $i$ th central tree is located.

**Evaluation of the optimal distance model for the spatial structure of forest stands**

*Importance of spatial structure parameters*

We applied the landscape ecology theory to understand patch homogeneity in terms the stand structure homogeneity by drawing on the existing research of natural forest stand structures (Paluch 2021; Weintraub and Cholaky 1991). This theory requires homogeneity within patches and different characteristics among adjacent patches. In particular, we employed data mining using the homogeneity index with each spatial structure parameter through the maximum mutual information coefficient (MIC) (Reshef et al. 2011) to derive the weights of each spatial structure parameter. This provides a theoretical basis for quantitative research on the factors influencing the spatial structure of natural conifer-broadleaved mixed forests under thinning.

The homogeneity index was derived by the multiplication and division method  $L(g)$  as follows:

$$L(g) = \frac{\frac{1+M(g)}{\sigma_m} \cdot \frac{1+S(g)}{\sigma_s} \cdot \frac{1+OP(g)}{\sigma_{op}}}{[1 + U(g)] \cdot \sigma_u \cdot [1 + C(g)] \cdot \sigma_c \cdot [1 + aCI(g)] \cdot \sigma_{aCI} \cdot [1 + W(g)] \cdot \sigma_w} \tag{3}$$

When calculating the distance, we defaulted to the same weight for each index, however in the actual application, the importance of the different indexes varied. We used the homogeneity spatial structure index with the importance of each parameter for the improved fuzzy analytic hierarchy process (FAHP), which was combined with the entropy weight method for the combined weight analysis to determine the importance of each parameter. The entropy method was then adopted to determine the objective weight of each spatial structure parameter, which is based on the index variability. The smaller the entropy value, the more information the index provides and the greater the role it plays in

**Table 3** Values and types of spatial structure parameters in the corrected plot

Central tree number	$M_{vc}$	$OP_v$	$H_v$	$W_v$	$C_v$	$U_v$	$aCI_v$
1	0.6481	0.6667	0.1111	0.6667	0.6667	0.3333	0.1014
3	0.6667	0.2222	0.6481	0.4444	0.8889	0.4444	0.2599
4	0.6667	0.0000	0.6667	0.3333	1.0000	0.0000	0.4444
5	0.5000	0.2000	0.5333	0.2000	1.0000	0.8000	0.5280
6	0.2500	0.4000	0.6667	0.6000	0.7000	1.0000	0.1601
7	0.4167	0.2000	0.6667	0.2000	1.0000	0.8000	0.5107
8	0.2000	0.2000	0.5000	0.4000	1.0000	0.2000	0.2974
....							
142	0.9200	0.2500	0.8333	0.2500	1.0000	0.5000	0.5402
143	0.7550	0.5000	0.5000	0.2500	0.5000	0.7500	0.5896
....							
Type of indicator	Maximal index	Maximal index	Maximal index	Intermediate index	Intermediate index	Miniature index	Miniature index

decision-making. This method ensures the high objectivity of the weights.

*Quantifying spatial structure parameters*

Each tree was considered as a point on the plane and a Voronoi diagram and Delaunay triangulation network were constructed using ArcGIS10.5 based on the location of each tree’s plane coordinates. The Voronoi diagram divides the sample site into multiple Voronoi polygons according to the closest attributes of the elements in the object set, with each Voronoi polygon containing only one central tree. The number of trees neighboring the central tree is equal to the number of sides of the Voronoi polygon surrounding the central tree (Fig. 1), and the location and number of neighboring trees is determined from the Voronoi polygon surrounding the stand.

Grey correlation analysis is a multivariate statistical method that reveals the correlation between multiple objectives with limited information. It has been applied in several fields, such as multi-parameter optimization and environment evaluations (Wang et al. 2019; Wen et al. 2022). Quantitative methods based on grey correlation analysis can therefore measure the correlation between factors in a grey system, reflecting the correlation of a certain objective with respect to the optimal objective. In this study, the number of trees neighboring the central tree and the characteristics of the stand’s own attributes were considered as a grey system, and the higher the grey correlation, the better the effect of this parameter set. The

number of nearest neighbors and nearest neighbor trees of the central tree were eventually determined by calculating the integrated weights and generating a weighted Voronoi diagram using the Weighted Voronoi Diagram tool in ArcGIS10.5. Table 3 reports the values determined for each spatial structure parameter.

The TOPSIS (technique for order preference by similarity to an ideal solution) model is essentially a comprehensive evaluation method that employs distance as an evaluation criterion and is commonly used in multi-objective decision analysis for finite scenarios (Behzadian et al. 2012; Çelikkilek and Tüysüz 2020). The level of development potential of each spatial structure is assessed by defining a measure in the target space and thus calculating the degree to which the target object is close to the positive ideal solution and deviates from the negative ideal solution. The optimal distance model realizes a comprehensive multi-indicator evaluation of forest spatial structure, and the ideal values can be set as maxima, minimum, intermediate value (Chai 2016). Among the seven indexes, maximal, miniature and intermediate index are 1, 0 and 0.5, respectively (Table 3). The data is normalized to the initial data for all types of indicators except the largest ones. The formula is as follows:

$$\hat{x}_i = \max(x_i) - x_i \tag{4}$$

$$\hat{x}_i = 1 - \frac{|x_i - x_{best}|}{M}, M = \max\{|x_i - x_{best}|\} \tag{5}$$

**Table 4** Degree of weighted correlation of each characteristic factor in the thinned forest plots

Thinning intensity (%)	Weighted correlation of diameter at breast height	Weighted correlation of tree height	Weighted correlation of crown width	Weighted correlation of crown length
0	0.31	0.18	0.30	0.21
10	0.30	0.15	0.36	0.19
15	0.26	0.17	0.35	0.22
20	0.24	0.17	0.29	0.29
25	0.28	0.19	0.29	0.23
30	0.27	0.16	0.36	0.21
35	0.25	0.16	0.41	0.18
Total critic weight	0.31	0.17	0.31	0.21

where,  $x_i(i=1, 2, 3, \dots, n)$  represented the value of the spatial structure parameter of the  $i$ th central tree.

When calculating the distance, we defaulted to the same weight for each indicator, yet in the actual problem, the importance of different indicators may vary. Therefore, in practical applications, we used the improved fuzzy hierarchy method combined with the entropy weight method to assign weights ( $W_j^*$ ) to the indicators and used the weights and standardized posterior series ( $y_{ij}$ ) to construct the weighted evaluation matrix ( $z_{ij}$ ). The formulae for determining the positive ideal solution ( $Z^+$ ) and the negative ideal solution ( $Z^-$ ) are as follows:

$$Z^+ = (Z_1^+, Z_2^+, \dots, Z_m^+) = \left( \max\{z_{11}, z_{21}, \dots, z_{n1}\}, \max\{z_{12}, z_{22}, \dots, z_{n2}\}, \dots, \max\{z_{1m}, z_{2m}, \dots, z_{nm}\} \right) \tag{6}$$

$$Z^- = (Z_1^-, Z_2^-, \dots, Z_m^-) = \left( \min\{z_{11}, z_{21}, \dots, z_{n1}\}, \min\{z_{12}, z_{22}, \dots, z_{n2}\}, \dots, \min\{z_{1m}, z_{2m}, \dots, z_{nm}\} \right) \tag{7}$$

The spatial structure comprehensive index is calculated as shown in Eq. 8:

$$S_i = \frac{\sqrt{\sum_{j=1}^m \{Z_j^- - z_{ij}\}^2}}{\sqrt{\sum_{j=1}^m \{Z_j^+ - z_{ij}\}^2} + \sqrt{\sum_{j=1}^m \{Z_j^- - z_{ij}\}^2}} \tag{8}$$

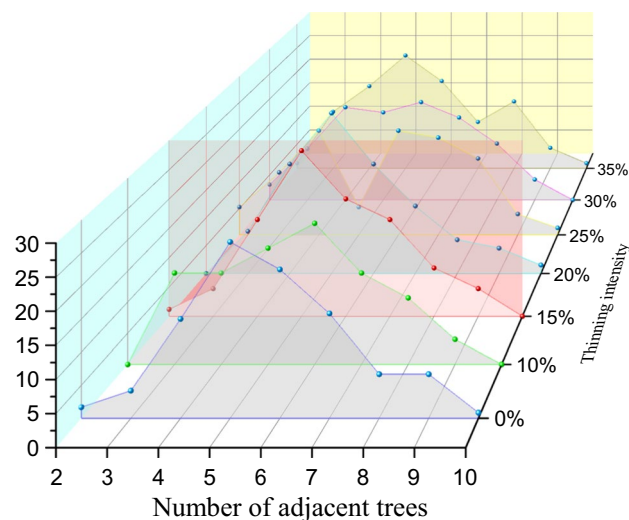


**Fig. 2** Frequency distance of the number of adjacent trees around the central tree based on the weighted Voronoi diagram

## Results

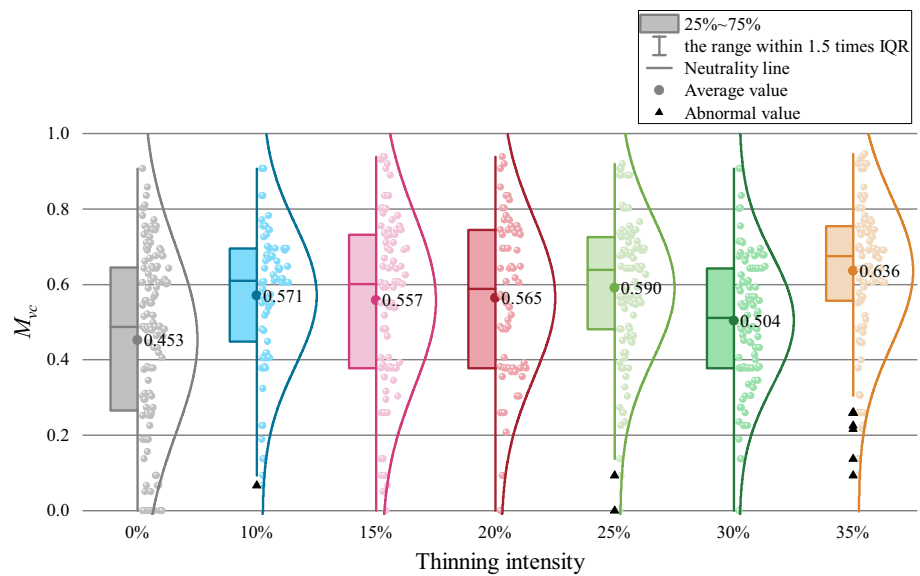
### Use of weighted grey correlation method to determine the spatial structure unit

The raw data of each characteristic factor for the 821 trees in the forest plot were processed without dimensions. The number of convex edges (i.e., number of adjacent trees) in the Voronoi diagram generated based on the tree point information for the corresponding 821 trees was analyzed in terms of diameter at breast height, height, crown length, and average crown width to obtain the weighted grey correlation for the spatial extent of tree competition.

The correlation trend was similar in the thinned sample plots, namely, the effect of crown width was greater than the effect of DBH, tree height, crown length. Moreover, the weighted correlation of crown width was between 0.29 and



**Fig. 3** Mingling degree value among different plots



0.41. This indicated that crown width had the greatest influence on the competitive range of trees among the four factors (Table 4). In single-species and stands with thinning exclusion, DBH and tree height generally exhibited a higher effect on the competitive unit. However, the canopy width was found to have the highest correlation with the competitive unit in thinned mixed conifer-deciduous stands due to species characteristics and management practices.

**Determination of the number of adjacent trees via weighted Voronoi diagrams**

The number of adjacent trees in each spatial structure unit was determined within the corrected forest plots based on weighted Voronoi diagrams, with a maximum of nine values

for all forest plots, ranging from two to 10 trees (Fig. 2). The distribution frequency of 3–8 adjacent trees in each plot was high, ranging from 90 to 96%; the distribution frequency of 2–3 adjacent trees did not exceed 14%; and 9–10 adjacent trees accounted for 4% to 6.6% in each thinned plot, which was lower than the plot with thinning exclusion. This may be attributed to the high sparseness and large distance between trees resulting from the forest plot thinning. In particular, the number of adjacent trees in the forest sites was reduced owing to the distance between the trees and the sparseness of the forest sites. Although the stand density of the forest plot with a thinning intensity of 10% was greater than that of the forest plot with a thinning intensity of 20%, the frequency distribution of stands with more than eight trees was less than that of the forest plot with a thinning intensity of 20%.

**Fig. 4** Neighborhood comparison values among different plots

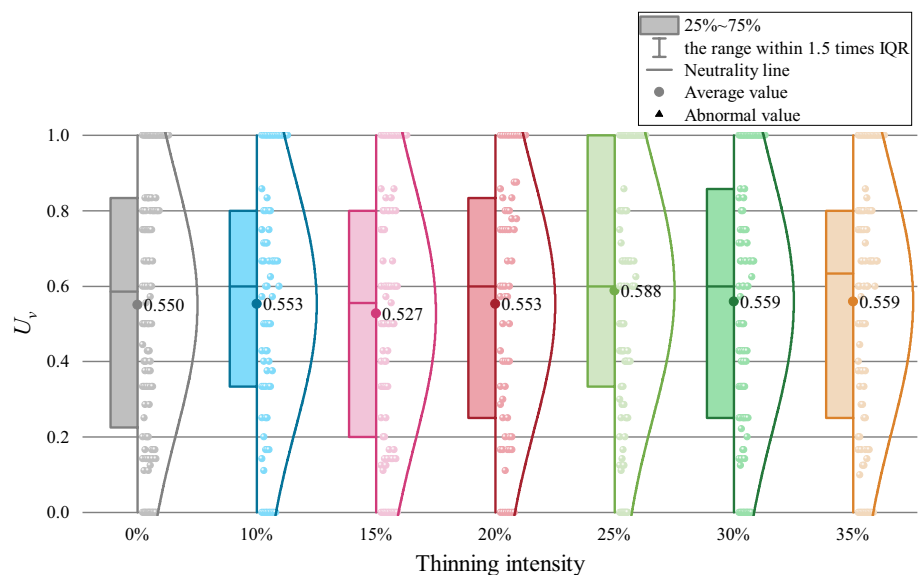
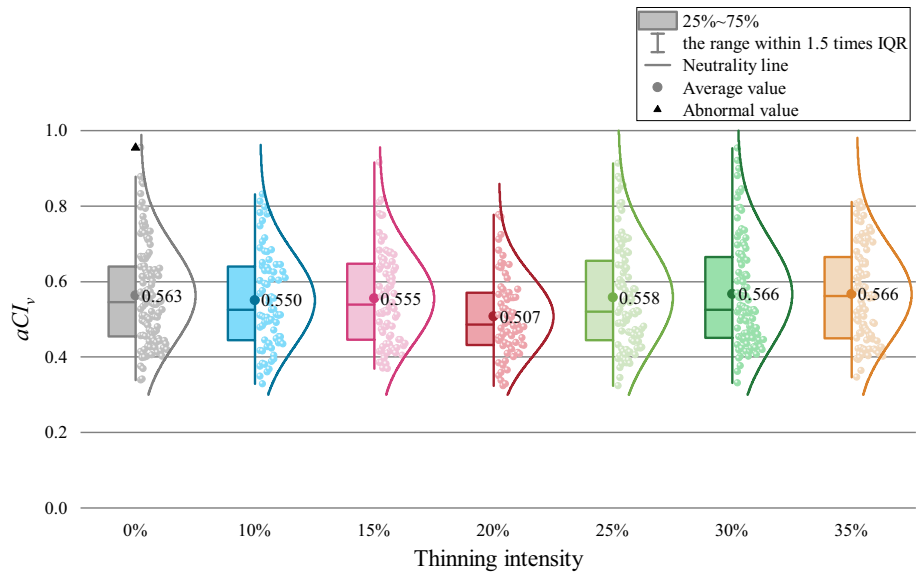


**Fig. 5** Competitive index values among different plots



This is linked to the distribution of the trees. The distance between the central and adjacent tree was predominantly found within the interval of the average crown width, demonstrating the applicability of the weighted Voronoi diagram for the analysis of thinned forest plots.

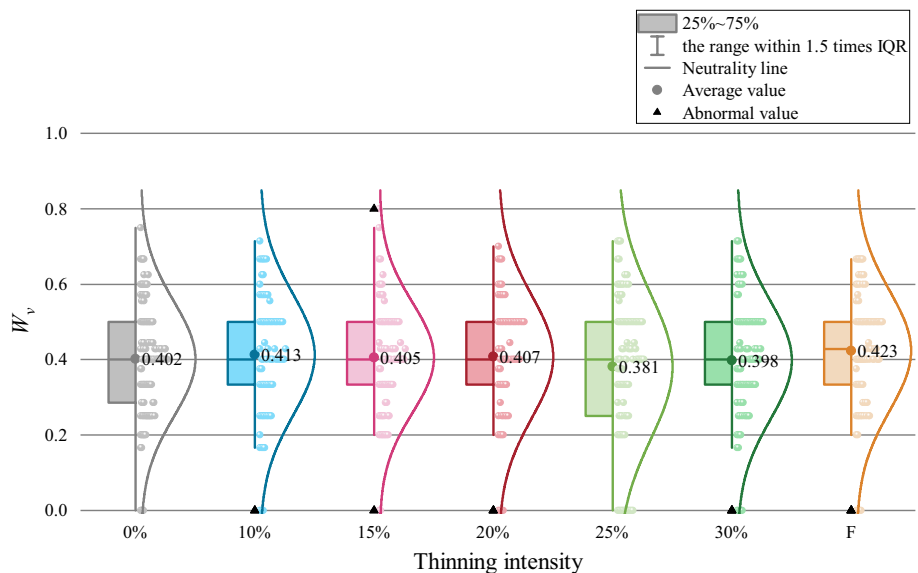
**Analysis of spatial structure parameters of forest stands**

*Degree of tree species segregation*

The median of the mingling degree in the thinning exclusion sample plot was determined as 0.488. Moreover, the median, 25% and 75% values of the thinned plots were higher than those of the thinning exclusion plot, and the median value was also greater than 0.5 (Fig. 3). The

difference of the lower and upper quartiles (IQR) of the thinned plots was smaller than that of the thinning exclusion plot. This reveals that a low dispersion degree of mingling in the thinned plots. Furthermore, the smallest fluctuation was observed as 0.198 for the sample plot with a 35% thinning intensity, indicating the superiority of the spatial structure of tree species in the thinned plots to that of the thinning exclusion plot. The degree of species mingling exceeded that in the plot with thinning exclusion, and the mingling degree of the sample plot with a thinning intensity of 35% was observed to be optimal among these plots. The degree of mingling in the thinning exclusion sample plot generally maintained an intermediate or low level (see Supplementary Material Tables S1–S8 for details of the mingling degree and other spatial structure

**Fig. 6** Uniform angle index value among different plots



parameters), and the degree of species mingling in the thinned sample plots was mainly strong or higher. In addition, the mingling frequency in each thinned sample plot was strong and extremely strong and the distribution frequencies ranged from 51.02 to 77.00%.

*Tree competition*

The mean value of the size ratio based on DBH was determined as ca. 0.50 (Fig. 4) in the thinned forest plots. For each structural unit, the distribution frequency of the central tree in the absolute inferior ( $U_v \in (0.75, 1.00]$ ) and predominant ( $U_v = 0.00$ ) states was determined to be the largest and smallest, respectively. The extremely inferior state was more common than the predominant state by 17.33%–26.80%.

The percentage of individuals in the inferior ( $U_v \in (0.50, 0.75]$ ) and extremely inferior ( $U_v \in (0.75, 1.00]$ ) states in the thinned forest plot was relatively large, reflecting the poor growth condition of the stands. The proportion of individuals in predominant, subdominant, intermediate, inferior, and extremely inferior stands in all plots exhibited a general increase, with the exception of forest plots with thinning intensities of 15% and 25%, where the proportion of stands in the inferior condition was observed to decrease. The forest plot with a thinning intensity of 15% had a clear dominance in the size ratio due to the uniform distribution of size ratios in the thinned forest sites under all classes.

The average value of the competition index in the thinned forest plots was determined as ca. 0.50 (Fig. 5). The majority of the trees were in an intermediate or strong competition

**Fig. 7** Open ratio index value among different plots

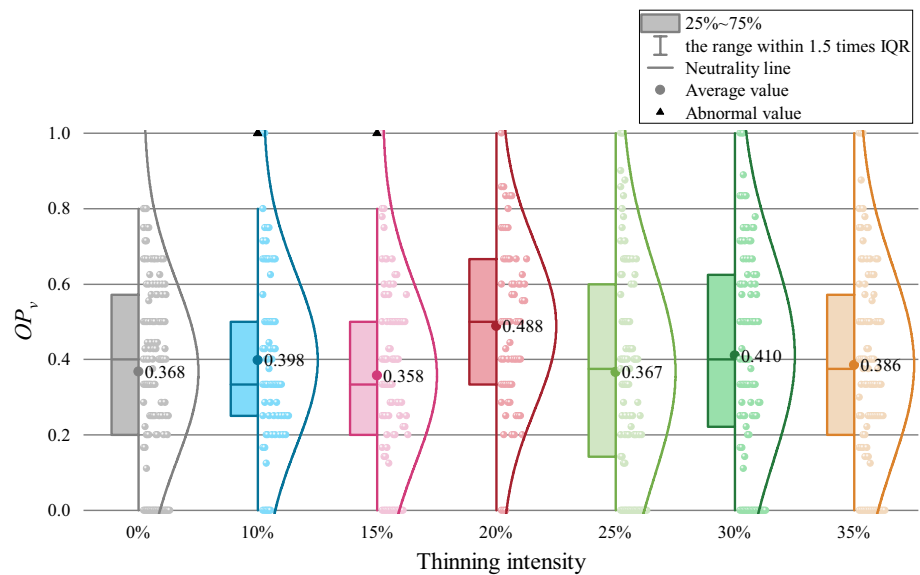
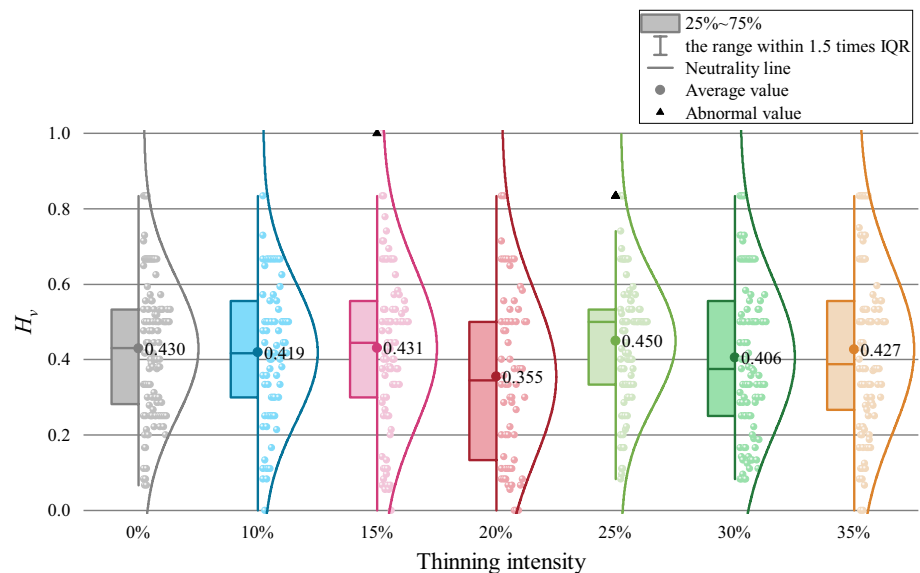


**Fig. 8** Stand layer index value among different plots



state, with the exception of forest plots with thinning intensities of 30% and 35%. The average competition index of these plots was lower than that of those with thinning exclusion. This may be attributed to the weak competition between trees caused by the reduced stand density via intermediate thinning. The competition value of the forest plot with a 20% thinning intensity was 0.323–0.778, with an average of 0.507. This indicates that the 20% intensity plot had a higher space utilization compared to the other sample plots.

*Spatial distribution pattern*

The frequency distribution trend of the spatial structure units for trees of different distribution states in each plot was relatively consistent, with an obvious normal distribution pattern (Fig. 6). Few trees belonged to the clumped distribution, (0–1%), while 2.35–12.37% belonged to the absolute uniform distribution. The majority of trees exhibited a random distribution (about 60%), and the distribution pattern of trees was relatively stable. Moreover, the largest number of stands belonged to the random distribution, accounting for about 60%, and the distribution pattern of stands was relatively stable. The mean values of all sample sites ranged from 0.381 to 0.423, and the mean angle with the 35% thinning intensity was closer to 0.5. However, the proportion with a random distribution was significantly smaller than that of plots with thinning intensities of 15% and 30%, and the proportion with a nonuniform distribution exceeded that of plots with thinning intensities of 15% and 30%. Thus, although the mean value of the angle with the 35% thinning intensity was larger, this is linked to the higher proportion of stands with a nonuniform distribution. Hence, the mean value cannot fully represent the level of the whole sample area.

*Degree of tree shade*

The openness ratio proportion was 31%–44% ( $OP_v = (0.25, 0.5]$ ) in all thinned plots, indicating that most of the tree units in the thinned stands of different intensities were in a intermediately open condition, namely, they were not entirely shaded (Fig. 7). However, the IQRs of forest plots with thinning intensities of 10%, 15% and 20% were 0.250, 0.300 and 0.334, respectively, which are smaller than those of the thinning exclusion plot. This reveals a lower dispersion degree for forest plots with thinning intensities of 10%, 15%, and 20%. Forest plot with the 20% thinning intensity exhibited the highest median and mean openness ratio values (0.500 and 0.488, respectively), and also the highest number of spatial units with intermediate openness (and above) and lowest frequency of shaded and fully shaded units in the stand (4.55% of fully shaded units). Thus, the open forest plot with a thinning intensity of 20% was optimal, with a sufficient growing space in the stand and favorable light environment.

The difference in stand stratification reflects the complexity of the stand in the vertical direction. The closer the forest layer difference index is to 1, the more complex the stand structure is in the vertical direction and the more obvious stratification is; the closer it is to 0, the more homogeneous the stand structure is. Figure 8 depicts the frequency distribution of stands under different stratification classes in each sample site, revealing a dominant normal distribution trend. Spatial structure units with an intermediate level were dominant in all the sample sites, followed by those with weak and strong vertical structures, while those with no difference and an extremely strong level were observed the least. Among them, the sample plot with 20% thinning intensity exhibited the most spatially structured units with no difference and

**Fig. 9** Crowding degree value among different plots

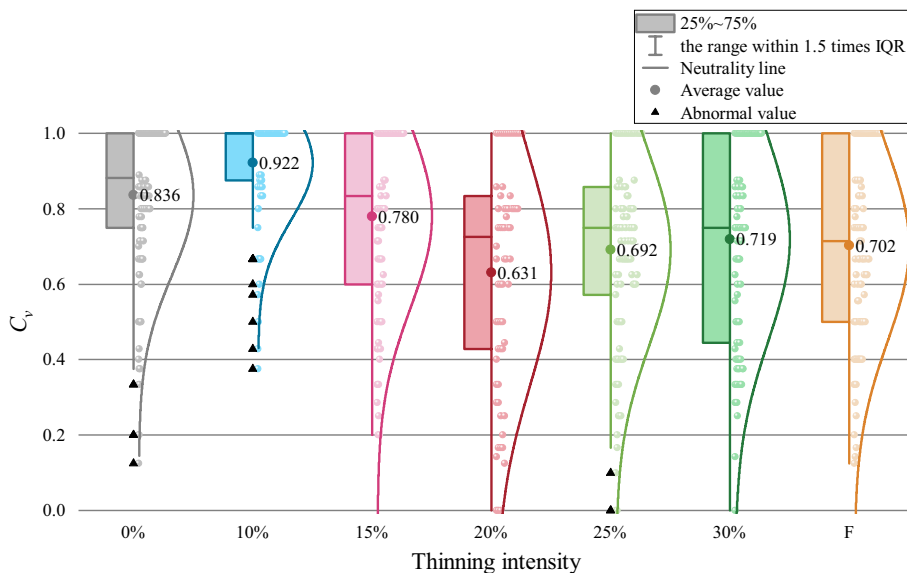


**Table 5** Consistency test results and weight of spatial structure parameters of natural conifer-broadleaved and broad-leaved mixed forest stands

Name	$U_v$	$aCI_v$	$W_v$	$M_{vc}$	$OP_v$	$H_v$	$C_v$
$U_v$	1	2	3	4	5	6	7
$aCI_v$	1/2	1	2	3	4	5	6
$W_v$	1/3	1/2	1	2	3	4	5
$M_{vc}$	1/4	1/3	1/2	1	2	3	4
$OP_v$	1/5	1/4	1/3	1/2	1	2	3
$H_v$	1/6	1/5	1/4	1/3	1/2	1	2
$C_v$	1/7	1/6	1/5	1/4	1/3	1/2	1
Consistency check	0000CR=0.02491; CI=0.0329						
Improved fuzzy hierarchical analysis weighting	0.350	0.237	0.159	0.106	0.070	0.046	0.032
Objective weights	0.23	0.04	0.05	0.06	0.17	0.08	0.37
Portfolio weighting	0.29	0.14	0.11	0.08	0.12	0.06	0.20

a weak vertical structure ( $H_v \leq 0.25$ ), with a frequency of nearly 35%, while the least was observed for the sample plot of 25% thinning intensity, with only 15.46%. In addition, the mean values for all sample sites from low to high thinning intensity were determined as 0.430, 0.419, 0.431, 0.355, 0.450, 0.406 and 0.427, respectively. At the stand level, the use of vertical space was similar for each thinning intensity, all of which exhibited a medium usage level and a vertical structure complexity degree close to the average. The forest layer difference in the sample plot with a thinning intensity of 20% was significantly different to those of the sample plot with a 25% thinning intensity ( $P < 0.05$ ), while no significant differences were observed for the rest of the sample plots ( $P > 0.05$ ). Thus, although the horizontal stratification of the different thinning stands is relatively similar, there are differences in the stratification within each thinning intensity and the vertical structural complexity of the spatial structural units of trees within the stand also varies.

The crowding degree means in the thinned plots (with the exception of the 10% thinning intensity sample plot) were lower than that of the thinning exclusion plot, ranging from 0.631 to 0.780 (Fig. 9). The majority of the trees in the 10% thinning intensity sample plot were in an extreme dense state (85.33%), while no trees were observed to be in an extreme sparse state. Moreover, the thinned plots exhibited a lower frequency of extreme dense trees compared to the thinning exclusion plot, with the exception of the 10% thinning intensity plot (40.91% – 58.82% frequency). This indicates that the effect of low thinning intensity on tree canopy growth cannot be ignored, although management measures of different thinning intensities have been carried out.

**Evaluation of integrated spatial structure indexes based on the optimal distance model**

*Parameter importance of spatial structure*

The importance analysis using the homogeneity spatial structure indexes of each structure parameter yielded the following ranking in descending order of importance:  $U_v$ ;  $aCI_v$ ;  $W_v$ ;  $M_{vc}$ ;  $OP_v$ ;  $H_v$ ; and  $C_v$ . The consistency test determined  $CR = 0.025$  (i.e.,  $< 0.1$ ) and  $CI = 0.03$ , which are acceptable values (Alanís-Anaya et al. 2017). Moreover, the entropy weighting analysis yielded objective weights for each structure parameter (Table 5), and the final combined weights were determined 0.29, 0.14, 0.11, 0.08, 0.12, 0.06 and 0.20 for  $U_v$ ,  $aCI_v$ ,  $W_v$ ,  $M_{vc}$ ,  $OP_v$ ,  $H_v$ , and  $C_v$ , respectively.

*Comprehensive evaluation and grade comparison of the spatial structure of forest stands*

The ranking of thinning intensities according to the optimal distance method was determined as 15% (0.488), followed by 20% (0.487), 30% (0.480), 25% (0.479), 10% (0.475), 0% (0.442), and, lastly, 35% (0.433). The evaluation index value of the forest plot with a thinning intensity of 35% was the lowest, differing by 0.009 from that of the thinning exclusion plot. Individual trees (51.67%) in the plot with thinning exclusion had moderate or less than moderate mingling, while forest plots with weak mingling dominated (20.83%). Extremely dense tree crowns and the strong competition level comprised 71.67% and 63.33% of the total, respectively. Trees in the extremely inferior state comprised 34.17%, and those with a moderately inferior level of the forest layer difference made up 68.33%. Moreover, 57.50% of trees were observed to have a random distribution. A total of 4.26% of trees from the 35% thinning intensity exhibited weak mingling, while 57.45% were inferior and extremely inferior, and 30% were relatively dense. Furthermore,

**Table 6** Comparison of the rationality evaluation of stand spatial structure

Plot	$M_{vc}$	$OP_v$	$H_v$	$W_v$	$C_v$	$U_v$	$aCI_v$	Grade evaluation	Distance model evaluation
0%	III	II	II	III	I	II	II	II	0.442
10%	IV	II	II	III	I	II	II	II	0.475
15%	IV	II	II	IV	II	II	II	III	0.488
20%	IV	III	II	III	II	II	III	III	0.487
25%	IV	II	II	III	II	II	II	III	0.479
30%	IV	II	II	IV	II	II	II	III	0.480
35%	IV	II	II	III	II	II	II	II	0.433

38.30% of the open stand ratio was observed at the shading and fully shading levels, 60.64% had strong or extremely strong competition, 67.02% had moderate and low forest layer levels, and 61.70% had randomly distributed stands, which were not significantly different from the thinning exclusion plot. The spatial structure of the above two forest stands with thinning intensities of 35% and thinning exclusion was poor.

In terms of the optimal spatial structure, 65% of the trees in the forest plot with a thinning intensity of 15% had a random distribution, and the subdominant level made up the majority, at 30%. Trees above the moderate state comprised ca. 71%, whereas 65% of trees were above the strong mingling level. For the 20% thinning intensity plot, 61% of trees were randomly distributed and the absolutely uniform was 4% higher than that of the 15% thinning intensity plot. In addition, the sum of the strongly mixed and extremely strongly mixed degree values was 62%, which is 3% lower than that of the 15% thinning intensity plot. Moreover, 17% were at the subdominant and above level, which is equal to that of the plot with a 15% thinning intensity. Furthermore, the plot with a 15% thinning intensity was less open than the 20% thinning intensity, yet its distribution of forest layer differences was higher. Although the percentage of trees in the plot with a thinning intensity of 15% at the extremely dense level (58.82%) was higher than in 20% thinning intensity plot (40.91%), the percentage at the strong competition (and above) level (46.97%) in the latter was lower than that of the former (62.35%). Moreover, the plot with a thinning intensity of 35% was extremely open (7.45%), had extremely strong forest layer variation (8.51%) and an extremely strong level of competition (9.57%), which were higher than those of the plot with a thinning intensity of 15%. However, their ranks accounted for a lower proportion of the total ranks. The 15% thinning intensity plot not only had a higher level of moderate openness (41.18%), moderate and upper forest layer variation (72.94%), and strong competition (55.29%) than the plot with a thinning intensity of 35%, but also had a higher proportion of ranks in the forest. In terms of mingling, the distribution of extremely mixed levels of mingling

was higher in the forest plot with a thinning intensity of 35% compared to that at the 15% intensity, yet the proportion of randomly distributed stands, subdominant and dominant ranks ( $U = [0, 0.25]$ ), and moderately mingled stands was lower.

The grade evaluation indicators of different plots corroborated the distance model value rankings (Table 6). Moreover, it expressed the disparity between the plots and fully utilized all data. The optimal solution distance model comprehensively combined the optimal distance and dominance of each parameter, which influenced the comprehensive evaluation of the spatial structure of forest stands. The forest plot with a 15% thinning intensity and 1000 ind. ha<sup>-1</sup> density exhibited the maximum index value, while the minimum value was observed for the forest plot with a 35% thinning intensity and 983 ind. ha<sup>-1</sup> density. The spatial structure and average neighborhood comparison based on DBH (Fig. 4) were optimized under the 15% thinning intensity. This indicates the DBH size ratio to be the main influencing factor of the spatial structure of natural conifer-broadleaved mixed forests. Performing standardization to facilitate comparisons among spatial structure indicators and evaluating the structure unit composition of each forest tree resulted in a more ideal optimal solution.

## Discussion

The results of mingling level, size ratio, competition index, and layer difference on the basis of Weighted Voronoi diagram are highly correlated with the traditional “1 + 4” adjacent tree method (Supplementary Material Figs. S1 and S2), indicating a high degree of consistency between the two methods. While the differences between the results of the two methods are relatively small, with 353–562 trees (55.59–88.50% of the total) being less than or equal to 0.1, the values of the angle, crowding, and openness determined by the weighted Voronoi diagram are significantly different from those calculated using the traditional “1 + 4” method (Fig. S1). About 355 trees have an angle index of greater

than or equal to 0.2, accounting for 55.91% of the total, and 359 trees have an openness index of greater than or equal to 0.2, accounting for 56.54% of the total. Comparing the results of the weighted Voronoi diagram with the standard Voronoi diagram shows that while the differences in mixed forest level, size ratio, competition index, angle-scale, and layer difference are relatively small, with 399–548 trees (62.83–86.30% of the total) being less than or equal to 0.1, there are notable differences between the values of the crowding and openness determined by the two methods (Fig. S2). Specifically, 283 trees have an openness index greater than 0.2, accounting for 44.57% of the total, and 282 trees have a crowding index greater than 0.2, accounting for 44.41% of the total. The weighted Voronoi diagram's ability to differentiate between various types or levels of tree importance through weight adjustment makes the analysis and decision-making process more targeted. The determination of the stand spatial structure unit is a prerequisite for forest spatial structure analysis. Adopting the traditional "1 + 4" adjacent tree method (1 central tree, 4 adjacent trees) or the conventional Voronoi diagram to analyze the spatial structure may exclude competing (i.e., adjacent) trees or include non-competing trees in a real stand (Cao et al. 2016). Based on the shortcomings of the "1 + 4" method, which often excludes adjacent trees, Mengping Tang et al. (2007), used the conventional Voronoi diagram to determine the basis of stand structure units, which ensured the maximum correlation between the central and adjacent trees and improved the accuracy of the results. However, the conventional Voronoi diagram only considered the spatial location of the forest trees when determining the adjacent trees and regarded all forest trees as stands with identical competitiveness, without considering the factors of the forest trees themselves, and often included non-competing trees. Thus, the constructed structure units could not truly reflect the actual range of influence of forest trees (Aakala et al. 2013). The most common physical impediments to interactions between stands are the crowding of the growing space and shading from above. Hence, in previous studies of pure stands, such interactions, were mainly dependent on the differences in the DBH, tree height, and crown width of adjacent stands. In this study, by considering the differences of tree species in conifer-broadleaved mixed natural forests, the Voronoi diagram method was modified to determine the structure unit of the forest based on the position information of the forest trees. This was combined with the four most critical factors affecting the competitive dynamics of the forest trees: crown width, DBH, crown length, and height.

The results of grey correlation analyses of the number of trees adjacent to the central tree and its key influencing factors showed that the average crown width of conifer-broadleaved mixed forests at each thinning intensity (i.e., 10%, 15%, 20%, 25%, 30% and 35%) had a greater influence

on the spatial extent of structure units when compared to the forest plot with thinning exclusion. In addition, the crown length factor had a stronger impact than the tree height. Previous research has demonstrated that the allocation of tree organs is strongly related to spatial partitioning and that tree growth increases with the acquisition of canopy space (Goudie et al. 2009; Abellanas et al. 2016; Moeur 1993). Our findings thus provide a theoretical basis for the scientific determination of the structure units of managed mixed conifer-broadleaved forests. We revealed the importance of determining tree structure units based on the weighted Voronoi diagram and validated the rationale for applying the weighted Voronoi diagram to thinned natural conifer-broadleaved mixed forests.

To clarify the influences of each parameter on spatial structure, the correlation between the spatial structure index (i.e., homogeneity structure index) obtained by the multiplication and division method and each parameter was determined. The spatial structure factors in conifer-broadleaved mixed forest stands were ranked in the following descending order of importance:  $U_i$ ;  $aCI_i$ ;  $W_i$ ;  $M_{ci}$ ;  $OP_i$ ;  $H_i$ ; and  $C_i$ . The optimal distance model was used to rank the size of the spatial structure. The proposed optimal distance model-based evaluation of stand spatial structure not only solves the importance and priority in calculating structure parameters but can also be adopted for the quantitative evaluation of stand spatial structure. The size ranking of the spatial structure index of the thinned forest plots was 15% (0.488), followed by 20% (0.487), 30% (0.480), 25% (0.479), 10% (0.475), 0% (0.442), and lastly 35% (0.433). According to the combined score of the optimal distance model, the spatial structure of the stand was optimized in the 15% thinning intensity plot. This plot exhibited a high proportion of trees at the moderately open level (41.18%), with moderate and upper stand variation (72.94%), and a strong level of competition (55.29%). In terms of the mingling degree, the distribution of very intense mingling classes was higher in the forest plot with a 35% thinning intensity than the 15% thinning intensity plot, yet its share of randomly distributed stands, subdominant and dominant classes ( $U = [0, 0.25]$ ), and trees with a moderate degree of mingling were lower. Forest plots with a better stand structure were those under the thinning intensities of 15% and 20%, which were more ecologically vigorous owing to the large degree of mingling, suitable size differentiation, and competition. Moreover, the whole stand was more ecologically vigorous, whereas the plots under 35% thinning exhibited weak mingling, a simple structure in the vertical direction, lacked young trees in the lower layer, and had a poor overall stability. Structured management has become a common forest management model in the last decade, and stand structure plays a decisive role in the development of forest functions. Natural secondary forests are prone to be over-dense and rely only on the natural

thinning of the stand, which has a very slow growth rate, an unreasonable structure and is unfavorable to the growth of light-loving tree species (Zhao 2021; Hu et al. 2020; Makana and Thomas 2005; Canham et al. 2004). Anthropogenic disturbance in forests has an impact on the spatial structure of a stand (Li et al. 2014; Xu et al. 2018; Montoro Girona et al. 2019; Hiltner et al. 2018). The crown crowding in the study area was high, and consequently requires reasonable management. Therefore, following our evaluation of the spatial structure of mixed conifer-broadleaved natural forests, we recommend the careful consideration of the contribution of each spatial structure parameter and the determination of the priority adjustment according to its stand rank.

## Conclusion

The results are highly correlated and consistent when calculating the mingling, size ratio, competition index, layer difference. However, the results of the calculation of angle, crowding and openness differed considerably between the two. Most of the angle and crowding values were smaller and the openness values were higher those determined with the traditional calculation. However, the Delaunay triangle network structure itself better reflects the distribution pattern of individuals on the horizontal ground, and the spatial structure of the stand based on Weighted Voronoi diagrams and Delaunay triangle networks does not require distance measurement and angle measurement between the central tree and its neighbors.

The degree of competition and spatial distribution pattern were the main reasons for the differences in the spatial structure of thinning coniferous-broadleaved mixed forests. The DBH-based neighborhood comparison was identified as the main contributing parameter to the degree of competition, while crowding was observed to be the key influencing factor of the tree shade degree. Based on the combination Weight-TOPSIS method, a spatial structure evaluation model was established for seven plots after selection for harvest. The proposed method was able to accurately and scientifically evaluate the spatial structure of the stands. Furthermore, the parameter scores of the evaluation model could be used to distinguish the degree of mingling, competition, spatial distribution pattern and tree shade degree of each mixed forest under different thinning intensities. The results provide a theoretical basis for the forest management of natural coniferous-broadleaved mixed forests, and offer a novel approach for the scientific evaluation of coniferous-broadleaved mixed forests with different thinning intensities.

Forest stand spatial structure research is increasingly moving towards comprehensive evaluation, however, forest structure is very complex, and the integrated evaluation method of optimal solution distance explored and

established in this paper, although it has a certain evaluation effect on spatial structure, is only compared and analyzed by each structural parameter and integrated evaluation index with traditional calculation results because the degree of difference of its quantitative index is not unified. Therefore, further research is needed for the subsequent characterization of the integrated quantitative degree.

**Acknowledgements** We thank members of the Dongfanghong Forest Farm for their assistance in the field. We also acknowledge Tian Zhang and Hangfeng Qu for their invaluable review of this manuscript.

**Open Access** This article is licensed under a Creative Commons Attribution 4.0 International License, which permits use, sharing, adaptation, distribution and reproduction in any medium or format, as long as you give appropriate credit to the original author(s) and the source, provide a link to the Creative Commons licence, and indicate if changes were made. The images or other third party material in this article are included in the article's Creative Commons licence, unless indicated otherwise in a credit line to the material. If material is not included in the article's Creative Commons licence and your intended use is not permitted by statutory regulation or exceeds the permitted use, you will need to obtain permission directly from the copyright holder. To view a copy of this licence, visit <http://creativecommons.org/licenses/by/4.0/>.

## References

- Aakala T, Fraver S, D'Amato AW, Palik BJ (2013) Influence of competition and age on tree growth in structurally complex old-growth forests in northern Minnesota, USA. *For Ecol Manage* 308:128–135. <https://doi.org/10.1016/j.foreco.2013.07.057>
- Abedi R (2022) Application of multi-criteria decision making models to forest fire management. *Int J Geohelit Parks* 10(1):84–96. <https://doi.org/10.1016/j.ijgeop.2022.02.005>
- Abellanas B, Abellanas M, Pommerening A, Lodaes D, Cuadros S (2016) A forest simulation approach using weighted Voronoi diagrams. An application to Mediterranean fir *Abies pinsapo* Boiss stands. *For Syst* 25(2):e062. <https://doi.org/10.5424/fs/201652-08021>
- Alanís-Anaya RM, Legorreta-Paulín G, Mas JF, Granados-Ramírez GR (2017) Susceptibility to gravitational processes due to land cover change in the Río Chiquito-Barranca del Muerto subbasin (Pico De Orizaba Volcano, México). *J Mountain Sci* 14(12):2511–2526. <https://doi.org/10.1007/s11629-016-4268-9>
- Behzadian M, Khanmohammadi Otaghsara S, Yazdani M, Ignatius J (2012) A state-of-the-art survey of TOPSIS applications. *Expert Syst Appl* 39(17):13051–13069. <https://doi.org/10.1016/j.eswa.2012.05.056>
- Brang P (2005) Virgin forests as a knowledge source for central European silviculture: reality or myth. *For Snow Landsc Res* 79(1/2):19–32
- Canham CD, LePage PT, Coates KD (2004) A neighborhood analysis of canopy tree competition: effects of shading versus crowding. *Can J for Res* 34(4):778–787. <https://doi.org/10.1139/x03-232>
- Cao X, Li J (2016) Research progress on indicators of the stand spatial structure. *For Resour Manage*. <https://doi.org/10.13466/j.cnki.lyzygl.2016.04.013>
- Cao XY, Li J, Chen L, Hu Y (2016) Intraspecific and interspecific competition analysis of *Cunninghamia lanceolata* ecological forest based on weighted Voronoi diagram. *Chin J Ecol* 35(09): 2553–2561. <https://doi.org/10.13292/j.1000-4890.201609.029>



- Cascone T, William WN Jr, Weissferdt A, Leung CH, Lin HY, Pataer A, Godoy MCB, Carter BW, Federico L, Reuben A, Khan MAW, Dejima H, Francisco-Cruz A, Parra ER, Solis LM, Fujimoto J, Tran HT, Kalthor N, Fossella FV, Mott FE, Tsao AS, Blumenschein G Jr, Le X, Zhang J, Skoulidis F, Kurie JM, Altan M, Lu C, Glisson BS, Byers LA, Elamin YY, Mehran RJ, Rice DC, Walsh GL, Hofstetter WL, Roth JA, Antonoff MB, Kadara H, Haymaker C, Bernatchez C, Ajami NJ, Jenq RR, Sharma P, Allison JP, Futreal A, Wargo JA, Wistuba II, Swisher SG, Lee JJ, Gibbons DL, Vaporciyan AA, Heymach JV, Sepesi B (2021) Neoadjuvant nivolumab or nivolumab plus ipilimumab in operable non-small cell lung cancer: the phase 2 randomized NEOSTAR trial. *Nat Med* 27(3):504–514. <https://doi.org/10.1038/s41591-020-01224-2>
- Çelikkbilek Y, Tüysüz F (2020) An in-depth review of theory of the TOPSIS method: an experimental analysis. *J Manage Anal* 7(2):281–300. <https://doi.org/10.1080/23270012.2020.1748528>
- Chai Z (2016) Quantitative evaluation and R programming of forest spatial structure based on the relationship of neighborhood trees: a case study of typical secondary forest in the mid-altitude zone of the Qinling Mountains. Dissertation, Northwest A&F University
- Chen G, Dai L, Ji L, Deng H, Hao Z, Wang Q (2004) Assessing forest ecosystem health I. Model, method, and index system. *Chin J Appl Ecol* 10:1743–1749. <https://doi.org/10.3321/j.issn:1001-9332.2004.10.008>
- Dong L, Bettinger P, Liu Z (2022) Optimizing neighborhood-based stand spatial structure: four cases of boreal forests. *For Ecol Manage* 506:119965. <https://doi.org/10.1016/j.foreco.2021.119965>
- dos Santos BM, Godoy LP, Campos LMS (2019) Performance evaluation of green suppliers using entropy-TOPSIS-F. *J Clean Prod* 207:498–509. <https://doi.org/10.1016/j.jclepro.2018.09.235>
- Duchateau E, Schneider R, Tremblay S, Dupont-Leduc L, Pretzsch H (2021) Modelling the spatial structure of white spruce plantations and their changes after various thinning treatments. *Forests* 12(6):740. <https://doi.org/10.3390/f12060740>
- Gauthier M-M, Tremblay S (2019) Late-entry commercial thinning effects on *Pinus banksiana*: growth, yield, and stand dynamics in Québec. *Canada J for Res* 30(1):95–106. <https://doi.org/10.1007/s11676-018-0778-3>
- Goudie JW, Polsson KR, Ott PK (2009) An empirical model of crown shyness for lodgepole pine (*Pinus contorta* var. *latifolia* [Engl.] Critch.) in British Columbia. *For Ecol Manage* 257(1): 321–331. <https://doi.org/10.1016/j.foreco.2008.09.005>
- Hiltner U, Huth A, Bräuning A, Héroult B, Fischer R (2018) Simulation of succession in a neotropical forest: high selective logging intensities prolong the recovery times of ecosystem functions. *For Ecol Manage* 430:517–525. <https://doi.org/10.1016/j.foreco.2018.08.042>
- Horner GJ, Baker PJ, Nally RM, Cunningham SC, Thomson JR, Hamilton F (2010) Forest structure, habitat and carbon benefits from thinning floodplain forests: Managing early stand density makes a difference. *For Ecol Manage* 259(3):286–293. <https://doi.org/10.1016/j.foreco.2009.10.015>
- Hu J, Herbohn J, Chazdon RL, Baynes J, Vanclay JK (2020) Long-term growth responses of three *Flindersia* species to different thinning intensities after selective logging of a tropical rainforest. *For Ecol Manage* 476:118442. <https://doi.org/10.1016/j.foreco.2020.118442>
- Hui G, Zhang G, Zhao Z, Yang A (2019) Methods of forest structure research: a review. *Curr for Rep* 5(3):142–154. <https://doi.org/10.1007/s40725-019-00090-7>
- Hui G, Hu Y, Zhao Z, Yuan S, Liu W (2013) A forest competition index based on intersection angle. *Sci Silvae Sin* 49(06): 68–73. <https://doi.org/10.11707/j.1001-7488.20130610>
- Irfan M, Elavarasan RM, Ahmad M, Mohsin M, Dagar V, Hao Y (2022) Prioritizing and overcoming biomass energy barriers: Application of AHP and G-TOPSIS approaches. *Technol Forecast Soc Change* 177: 121524. <https://doi.org/10.1016/j.techfore.2022.121524>
- Knocke T, Ammer C, Stimm B, Mosandl R (2008) Admixing broadleaved to coniferous tree species: a review on yield, ecological stability and economics. *Eur J for Res* 127(2):89–101. <https://doi.org/10.1007/s10342-007-0186-2>
- Li F (2019) Forest mensuration. China Forestry Publishing Press, Beijing
- Li J, Zhang H, Liu S, Kuang Z, Wang C, Zang H, Cao X (2013) A space optimization model of water resource conservation forest in Dongting Lake based on improved PSO. *Acta Ecol Sin* 33(13):4031–4040. <https://doi.org/10.5846/stxb201207281072>
- Li Y, Ye S, Hui G, Hu Y, Zhao Z (2014) Spatial structure of timber harvested according to structure-based forest management. *For Ecol Manage* 322:106–116. <https://doi.org/10.1016/j.foreco.2014.02.042>
- Li J, Fang X, Feng R, Sun H, Cao X, Zhao C, Li J (2015) Tree competition indexes based on weighted Voronoi diagram. *J Beijing For Univ* 37(03): 61–68. <https://doi.org/10.13332/j.1000-1522.20140310>
- Li X, Zhang G, Li J (2020) Spatial structure evaluation of natural secondary forest around Dongting lake based on entropy weight-cloud model. *J Coastal Res* 103(SI): 484–489
- Lodin I, Brukas V (2021) Ideal vs real forest management: Challenges in promoting production-oriented silvicultural ideals among small-scale forest owners in southern Sweden. *Land Use Pol* 100:104931. <https://doi.org/10.1016/j.landusepol.2020.104931>
- Lv Y, Zang H, Wan X, Deng Z, Li J (2012) Storey structure study of *Cyclobalanopsis myrsinaefolia* mixed stand based on storey index. *For Resour Manage*. <https://doi.org/10.13466/j.cnki.lyzygl.2012.03.023>
- Makana JR, Thomas SC (2005) Effects of light gaps and litter removal on the seedling performance of six african timber species I. *Biotropica* 37(2):227–237. <https://doi.org/10.1111/j.1744-7429.2005.00030.x>
- Moeur M (1993) Characterizing spatial patterns of trees using stem-mapped data. *For Sci* 39(4):756–775. <https://doi.org/10.1093/forests/39.4.756>
- Montoro Girona M, Morin H, Lussier JM, Ruel JC (2019) Post-cutting mortality following experimental silvicultural treatments in unmanaged boreal forest stands. *Front Plant Sci* 2:4. <https://doi.org/10.3389/ffgc.2019.00004>
- Nagel TA, Zenner EK, Brang P (2013) Research in old-growth forests and forest reserves: implications for integrated forest management. In: G Brunialti (eds) Integrative approaches as an opportunity for the conservation of forest biodiversity. European Forest Institute, Freiburg
- Nagel TA, Svoboda M (2008) Gap disturbance regime in an old-growth *Fagus-Abies* forest in the Dinaric Mountains, Bosnia-Herzegovina. *Can J For Res* 38(11):2728–2737. <https://doi.org/10.1139/X08-110>
- Palczewski K, Sałabun W (2019) The fuzzy TOPSIS applications in the last decade. *Proc Comput Sci* 159:2294–2303. <https://doi.org/10.1016/j.procs.2019.09.404>
- Paluch J (2021) The stochastic backward shifts model better corresponds to the fine-scale structural heterogeneity of old-growth *Abies-Fagus-Picea* forests than the ontogenic life cycle model. *For Ecol Manage* 486:118978. <https://doi.org/10.1016/j.foreco.2021.118978>
- Pommerening A (2006) Evaluating structural indices by reversing forest structural analysis. *For Ecol Manage* 224(3):266–277. <https://doi.org/10.1016/j.foreco.2005.12.039>
- Qiao X, Huang H, Shi X (2020) Agricultural environmental efficiency, environmental harmonization and influencing factors

- of major grain-producing areas in china: from the constrained perspective of carbon emission. *Int J Soc Sci Univ* 3(3):67–76
- Reshef DN, Reshef YA, Finucane HK, Grossman SR, McVean G, Turnbaugh PJ, Lander ES, Mitzenmacher M, Sabeti PC (2011) Detecting novel associations in large data sets. *Science* 334(6062):1518–1524. <https://doi.org/10.1126/science.1205438>
- Solangi YA, Cheng LS, Shah SAA (2021) Assessing and overcoming the renewable energy barriers for sustainable development in Pakistan: an integrated AHP and fuzzy TOPSIS approach. *Renew Energy* 173:209–222. <https://doi.org/10.1016/j.renene.2021.03.141>
- Song Q, Dong X (2014) Comprehensive evaluation of forest community stability of different types of low-quality forest stands in the greater Hignnan Mountains. *Sci Silvae Sin* 50(6): 10–17. <https://doi.org/10.11707/j.1001-7488.20140602>
- Sun Y (2007) Research on grey incidence analysis and its application. Dissertation, Nanjing University of Aeronautics and Astronautics
- Tang M, Chen Y, Shi Y, Zhou G, Zhao M (2007) Intraspecific and interspecific competition analysis of community dominant plant populations based on Voronoi diagram. *Acta Ecol Sin* 11:4707–4716. <https://doi.org/10.3321/j.issn:1000-0933.2007.11.039>
- Tang M, Zhou G, Chen Y, Zhao M, He Y (2009) Mingling of evergreen broad-leaved forests in Tianmu Mountain based on Voronoi diagram. *Sci Silvae Sin* 45(06):1–5
- Wang L, Li Z (2004) Distance-distinguish evaluation on environmental quality of Urban Parks in Wuhu. *J Anqing Norm Univ (Nat Sci Ed)* 1:66–69. <https://doi.org/10.3969/j.issn.1007-4260.2004.01.026>
- Wang G, Li WL, Rao F, He ZR, Yin ZP (2019) Multi-parameter optimization of machining impeller surface based on the on-machine measuring technique. *Chin J Aeronaut* 32(08):2000–2008. <https://doi.org/10.1016/j.cja.2018.09.005>
- Weintraub A, Cholaky A (1991) A hierarchical approach to forest planning. *For Sci* 37(2):439–460. <https://doi.org/10.1093/forestscience/37.2.439>
- Wen P, Li L, Xue H, Jia Y, Gao L, Li R, Huo L (2022) Comprehensive evaluation method of the poultry house indoor environment based on gray relation analysis and analytic hierarchy process. *Poult Sci* 101(2):101587. <https://doi.org/10.1016/j.psj.2021.101587>
- Xin Y, Zhu Q, Luo S, Gou Q (2020) Spatial structure characteristics of soil and water conservation forest in the loess area of northern Shaanxi. *Sci Soil Water Conserv* 18(05): 17–25. <https://doi.org/10.16843/j.sswc.2020.05.003>
- Xu L, Shi Y, Zhou G, Xu X, Liu E, Zhou Y, Zhang F, Li C, Fang H, Chen L (2018) Structural development and carbon dynamics of Moso bamboo forests in Zhejiang Province, China. *For Ecol Manage* 409:479–488. <https://doi.org/10.1016/j.foreco.2017.11.057>
- Yang M, Cai T, Ju C, Zou H (2019) Evaluating spatial structure of a mixed broad-leaved/Korean pine forest based on neighborhood relationships in Mudanfeng National Nature Reserve. *China J Forestry Res* 30(04):1375–1381. <https://doi.org/10.1007/s11676-019-00899-9>
- Yang L, Shi L, Wei J, Wang Y (2021) Spatiotemporal evolution of ecological environment quality in arid areas based on the remote sensing ecological distance index: a case study of Yuyang district in Yulin city. *China Open Geosci* 13(1):1701–1710. <https://doi.org/10.1515/geo-2020-0328>
- Ye S, Zheng Z, Diao Z, Ding G, Bao Y, Liu Y, Gao G (2018) Effects of thinning on the spatial structure of *Larix principis-rupprechtii* plantation. *Sustainability* 10(4):1250. <https://doi.org/10.3390/su10041250>
- Zhang Y, Fang S, Tian Y, Wang L, Lv Y (2022) Responses of radial growth, wood density and fiber traits to planting space in poplar plantations at a lowland site. *J For Res* 33(3):963–976. <https://doi.org/10.1007/s11676-021-01382-0>
- Zhang B, Dong X, Qu H, Gao R, Mao L (2023) Effects of thinning on ecosystem carbon storage and tree-shrub-herb diversity of a low-quality secondary forest in NE China. *J For Res* 34(4):977–991. <https://doi.org/10.1007/s11676-022-01531-z>
- Zhao X (2021) Research progress on natural forest regeneration. *World J For* 10(01): 33–42. <https://doi.org/10.12677/WJF.2021.101005>

**Publisher's Note** Springer Nature remains neutral with regard to jurisdictional claims in published maps and institutional affiliations.